UC Davis
UC Davis Previously Published Works

Title

Seasonal patterns of callose deposition and xylem embolism in five boreal deciduous tree species

Permalink

Journal

American Journal of Botany, 108(8)

ISSN

0002-9122

Authors

Miller, Ashley E
Stanfield, Ryan C
Hacke, Uwe G

Publication Date

2021-08-01

DOI

10.1002/ajb2.1718

Copyright Information

Peer reviewed

BRIEF COMMUNICATION

Botany
American Journal of
BOTANICAL SOCIETY OF AMERICA
leading research and education
since 1893

Seasonal patterns of callose deposition and xylem embolism in five boreal deciduous tree species

Ashley E. Miller[1] | Ryan C. Stanfield[2] | Uwe G. Hacke[1]

[1]Department of Renewable Resources, University of Alberta, Edmonton, AB, Canada

[2]Department of Viticulture and Enology, University of California Davis, Davis, CA, USA

Correspondence
Uwe G. Hacke, Department of Renewable Resources, University of Alberta, 442 Earth Sciences Building, Edmonton, AB T6G 2E3, Canada.
Email: uwe.hacke@ualberta.ca

Abstract

Premise: Phloem tissue allows for sugar transport along the entirety of a plant and, thus, is one of the most important anatomical structures related to growth. It is thought that the sugar-conducting sieve tube may overwinter and that its cells persist multiple seasons in deciduous trees. One possible overwintering strategy is to build up callose on phloem sieve plates to temporarily cease their function. We tested the hypothesis that five deciduous tree species produce callose on their sieve plates on a seasonal basis.

Methods: Young shoots of five deciduous tree species were sampled periodically between April 2019 and February 2020 in Edmonton, Alberta, Canada. After enzymatic digestion of cytoplasmic constituents, cross sections were imaged using scanning electron microscopy to observe and quantify the level of callose deposition at monthly intervals, and sieve plate pore size was measured. Using a conductivity apparatus, we measured xylem native embolism during these sampling periods.

Results: Contrary to past work on some of the same species, we found little evidence that sieve tubes overwinter by becoming occluded with callose. Instead, we found that most sieve plates remain open. Xylem embolism was minimal during the peak growing season, but increased over winter.

Conclusions: Many species had been assumed to deposit callose on sieve plates over winter, though anatomical and phenological phloem data were sparse. Our data do not support this notion.

KEYWORDS

anatomical phenology, beaked hazelnut (*Corylus cornuta*), boxelder maple (*Acer negundo*), callose, mountain ash (*Sorbus aucuparia*), phloem, quaking aspen (*Populus tremuloides*), red-osier dogwood (*Cornus sericea*), sieve plates, vascular transport

The phloem in vascular plants is widely known as the main food-conducting tissue (Evert, 2006), and thus is one of the most important anatomical structures related to growth. The phloem transports photoassimilates from source to sink, but it has various other functions as well (White, 2012; Saguez et al., 2013). Phloem sap flow is largely affected by the anatomy of the sieve plate (Thompson, 2006; Thompson and Wolniak, 2008; Truernit, 2014; Stanfield et al., 2019). The highest level of constriction within the fluidic channel occurs at sieve plate pores (Mullendore et al., 2010; Stanfield et al., 2019), which may be less than 0.5 μm in diameter (Thompson and Holbrook, 2003) and may become blocked with p-protein or callose (Zamski and Zimmerman, 1979; Furch et al., 2010; Zhang et al., 2012). Recent literature suggests that sieve plates contribute up to 85% of sieve tube

resistance (Mullendore et al., 2010; Stanfield et al., 2019), with oblong pores nearly doubling resistance when compared to round pores (Stanfield et al., 2019). Being the structure with the highest pathway resistance in the sieve tube, the sieve plate pores are the most influential in blocking off flow in response to external conditions. For example, sieve plates may become completely occluded with callose in as little as 20 min after injury (Mullendore et al., 2010). These restriction points in the sieve tube may provide a safety mechanism to prevent sap leakage after injury or to slow the spread of pathogens (Currier, 1957; Cronshaw and Esau, 1968, Ton and Mauch-Mani, 2004; De Schepper et al., 2010). The blockage of sieve plates may be modified dynamically by depositing and removing callose, a polysaccharide, in the apoplast surrounding the pore

(Eschrich, 1975), leading to changes in pore diameter and subsequent alterations in sap mass flow rate (Thompson and Holbrook, 2003). There is also evidence that callose deposition occurs to various degrees seasonally across multiple taxa (Esau, 1948; Evert, 1963; Alfieri and Evert, 1968; Zamski and Zimmermann, 1979; Montwé et al., 2019).

For over 140 years, phloem has been suggested to cease function temporarily during the winter and regain function during the spring (Wilhelm, 1880; Esau, 1948; McNairn and Currier, 1968; Chen and Kim, 2009; Bertoni, 2011; Fadón et al., 2020). Recently, Savage (2020) summarized different strategies of overwintered sieve tubes. Briefly, overwintered sieve tubes may either permanently close sieve plates and die or go into dormancy over winter and survive another season. In the first scenario, definitive callose is laid down on sieve plates, fully occluding sieve plate pores, but callose may later break down to leave little accumulation on the plate. In the second scenario, there are two potential outcomes: (1) the sieve plates remain relatively clear of blockage, or (2) dormancy callose accumulates over the winter and is removed when the sieve tube is reactivated in the spring.

Examples of dormancy callose are rare in the literature, although dormancy callose has been observed in some woody species such as *Vitis vinifera* and *Tecoma* species (Esau, 1948, 1950). When present, dormancy callose deposition generally begins in October, where callose is deposited on sieve plates of all stages of differentiation (Evert and Derr, 1964; Peel, 1974; Montwé et al., 2019). Come spring, specifically in April (Evert and Derr, 1964) or May (Aloni and Peterson, 1991), dormancy callose is removed from sieve elements that will function again a second year. By June (Aloni and Peterson, 1991) or July (Montwé et al., 2019), dormancy callose is almost completely removed from the sieve plates.

Recent studies suggest that (1) while dormancy callose does exist, sieve elements of dormant trees may never reach total occlusion by callose, and (2) consistent callose formation is not necessarily triggered by freezing temperatures (Prislan et al., 2018; Montwé et al., 2019), and (3) dormancy callose is not ubiquitous to all deciduous vascular plants, but its presence or absence appears to be associated with the timing of budbreak (Savage et al., 2020). For many species, it is yet to be discovered exactly when and how much dormancy callose is deposited on sieve plates seasonally and what external stimuli are responsible for this response. Further, it is unknown how callose deposition may impact the conductivity of sieve tubes, the velocity of phloem sap in overwintering phloem, and potential phloem translocation through winter dormancy (Savage, 2020).

Previous studies have shown that the species that we studied here exhibit varying methods of phloem overwintering. *Populus tremuloides* lays down definitive callose (Davis and Evert, 1968), while *Acer negundo* has not been reported to lay down definitive or dormancy callose (Tucker and Evert, 1969). To our knowledge, *Corylus cornuta,*

Sorbus aucuparia, and *Cornus sericea* have not been previously tested for overwintering callose. However, *Cornus sanguinea* does not lay down definitive callose, but may produce dormancy callose (Currier, 1957).

Knowledge of dormancy callose with regard to secondary phloem sieve plates is lacking, and in some cases remains preliminary (Truernit, 2014; Liesche et al., 2017; Savage, 2020). The present study aims to provide fundamental knowledge of secondary phloem sieve elements and sieve plates to better understand the seasonality of phloem in woody plants, particularly through dormancy in boreal regions. Filling this fundamental knowledge gap in tree physiology will help us better understand how trees survive in extraordinarily low temperatures during the winter and further recover in the spring.

The two long-distance transport systems, xylem and phloem, in vascular plants are rarely studied together (but see Pfautsch et al., 2015; Hillabrand et al., 2019; Montwe et al., 2019). Here, we measured seasonal variation in phloem callose deposition using a scanning electron microscope (e.g., Montwé et al., 2019), along with seasonal variation in xylem transport capacity using a conductivity apparatus (e.g., Sperry et al., 1988). Edmonton experiences long and cold winters; hence, we expected that woody vessel-bearing plants would experience relatively high levels of freezing-induced embolism (Sperry et al., 1988, Hacke and Sauter, 1996). Meanwhile, the phloem sap flow in winter may differ by species (e.g., *Salix exigua* has continued to translocate phloem sap at −13°C (Fisher, 1983), while *Salix viminalis* has been shown to discontinue translocation in temperatures below −4°C (Weatherley and Watson, 1969), causing a winter cessation of phloem activity (Eschrich, 1975). Because xylem and phloem are thought to be linked (Sevanto et al., 2011; Pfautsch et al., 2015; Salleo et al., 2006), we expected patterns of winter callose deposition to roughly match declines in xylem hydraulic conductivity.

There are many unknowns and seemingly conflicting information regarding the seasonal structure of phloem; namely when, to what extent and why dormancy callose is deposited. By taking physiological measurements across 9 months, we aimed to answer the following questions: (1) What percentage of sieve plates exhibit seasonal dormancy callose deposition per species? (2) Is there a seasonal pattern of callose deposition that parallels trends in xylem embolism? (3) Does the area of individual sieve plate pores differ between species, and if so, do differences in pore size correlate with trends in seasonal callose deposition?

MATERIALS AND METHODS

Phloem tissue collection for microscopy

Samples were collected approximately monthly from the Saskatchewan River valley within Kinsmen Park in Edmonton, Alberta, Canada (53°31′43.7″N 113°31′03.9″W)

between April 2019 and January 2020. The following five species were identified and collected at each date: (1) red-osier dogwood (*Cornus sericea* L.), (2) beaked hazelnut (*Corylus cornuta* Marshall), (3) mountain ash (*Sorbus aucuparia* L.), (4) boxelder maple (*Acer negundo* L.), and (5) quaking aspen (*Populus tremuloides* Michx.). For each species, samples were collected from three separate individuals and five sieve plates were imaged per sample, totaling 15 sieve plates per species on each sampling date. We avoided taking samples from the same individual at different dates to prevent the observation of wound callose rather than dormancy callose. Our sampling site was relatively confined (~0.2 km^2), and therefore, individuals experienced largely the same environmental conditions.

The collection process involved searching for the five species, and once an individual was identified, its overall health was visually assessed. Collections from healthy individuals were prioritized to minimize the chance of observing wound callose rather than dormancy callose. If there was apparent damage, such as possible bug or fungal infestation, or the tree looked to be in poor health displaying dying shoots, it was skipped. Once a healthy tree was found and identified as one of the five species of interest, a cutting of approximately 2 cm of a distal twig roughly 2 years old was taken, immediately submerged into 100% ethanol in a 2-mL microcentrifuge tube and placed into a container filled with 1 L of liquid nitrogen. Samples were removed from liquid nitrogen and placed into a –20°C freezer for at least 24 h.

Xylem tissue collection and conductivity measurements

All samples for the xylem conductivity measurements were collected between 09:00 and 11:00 hours at approximately breast height from distal twigs of healthy-looking shrubs and trees. Six twigs per species were measured (usually one twig per plant). Samples were placed in large plastic bags and were immediately brought to the laboratory, which was within walking distance to the study site. Within 90 min of collection, the cut ends of samples were successively cut underwater. The segments used for measurements were 14 cm long and at least 25 cm away from the original cut end.

After K_{native} was measured, segments were degassed underwater overnight in a vacuum to remove embolism, and hydraulic conductivity was re-measured to estimate the maximum hydraulic conductivity (K_{max}). Percentage maximum xylem conductivity was calculated as $(100/K_{max}) \times K_{native}$.

Laboratory processing for microscopy

The protocol for protein and cytoplasmic digestion followed that developed by Mullendore et al. (2010) to dissolve p-proteins on sieve plates and to hydrolyze any leftover starch. Briefly, samples were thawed, cut into 2-mm segments, submerged in a proteinase K digestion solution for 2 weeks on an Eppendorf ThermoMixer (Hamburg, Germany) at 55°C and 300 rpm. Samples were removed, washed, and submerged in an amylase solution at 60°C for 24 h. Finally, samples were lyophilized for 24 h using a LABCONCO FreeZone 2.5 Liter Benchtop Freeze Dryer (Kansas City, MO, USA). The result was sieve plates clear of wound-related callose (freeze substitution, see above) and free from cytoplasmic constitutes that would block reliable view of sieve plates.
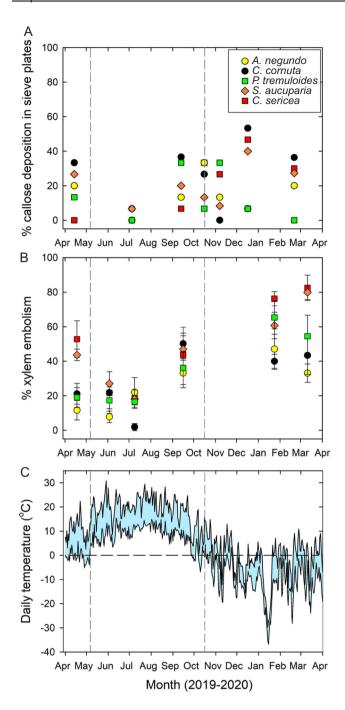
Scanning electron microscopy

Lyophilized samples were mounted onto aluminum specimen mounts with Ted Pella carbon Pelco tabs (Redding, CA, USA), sputter-coated with gold using a Nanoscience Instruments SEMPrep 2 (Phoenix, AZ, USA) sputter coater set to 1500 V for 1.5 min, and loaded into a Zeiss Sigma 300 VP Field Emission Scanning Electron Microscope (Oberkochen, Germany) set to 10 kV accelerating voltage, using a Secondary Electron Detector (SE2) beam with a working distance between 7–8 mm.

Phloem tissue was located, and magnification was set to ensure that the complete phloem tissue was in view, from the inner vascular cambium to the outer surrounding phloem fibers. This was done to prevent collection bias from any one location in the phloem, as there is potential for cambial phloem to still be in development and not representative of mature phloem. Phloem tissue was scanned until a sieve plate was observed, which was then magnified and imaged. The first five plates observed per sample were used. A plate was only skipped if it was deemed unreliable to categorize due to damage or undigested proteins, for example. Sieve plates were categorized into the following categories: (1) no callose present—less than approximately 10% of callose deposition observed on a plate, (2) callose present—signs of callose deposition leading to visible occlusion (>10% callose deposition on a plate). All data were collected by one individual to remain consistent with categorization and to minimize bias.

Calculation of pore size per species

Length and width of sieve plate pores were found by measuring the approximate longest distance across a pore in

The native hydraulic conductivity of the xylem (K_{native}) was measured using a conductivity apparatus (Sperry et al., 1988; Hacke et al., 2000; Schreiber et al., 2011) with a pressure head of 4 kPa. Most of the segments used in this study had one or two xylem rings and had an average xylem area (excluding pith) of 11.1 mm^2. The average xylem area per species varied from 10.2 mm^2 in mountain ash to 12.0 mm^2 in hazelnut.

FIGURE 1 Seasonal dynamics of callose deposition on sieve plates and xylem embolism in twigs of five boreal species tested from April 2019 to March 2020. (A) Percentage of sieve plates with notable callose deposition. Sieve plates were observed using a field emission scanning electron microscope (FESEM). Symbols are means of 75 sieve plates per sampling date. In this study, "no callose deposition" is defined as less than approximately 10% callose coverage per plate. (B) Mean (±SE) percentage xylem embolism in six stem segments per species. The mean native embolism was minimal during the peak growing season but increased later in the growing season and peaked during winter. (C) Maximum and minimum daily temperatures during the sampling dates. The range is highlighted in blue. The dashed vertical lines represent the approximate dates of leaf drop (mid-October) and leaf flush (early May). These dates were similar for all five species

pixels and taking a perpendicular transect for the shortest distance using ImageJ (Bethesda, MD, USA) software. Values were recorded and converted into micrometers by calculating the ratio of micrometers to pixels using the image's scale bar, then multiplying the ratio to each long and short segment. Sieve plate pores were assumed to be elliptical for approximate area calculations. Pore area (μm^2) was calculated using the formula for the area (A) of an ellipse: $A = ab\pi$, where a is the semi-major axis (length) and b is semi-minor axis (width) of the pore. Further, the ratio of the mean minor axis (μm) to the mean major axis (μm) was calculated represent "roundness".

Statistical analyses

All statistical analyses were carried out in R 4.0.0 (R Core Team, Vienna, Austria). Significance level was set to $p \le 0.05$. Species data from Figure 1A was aggregated into one of two categories based upon the occurrence of freezing temperatures: summer or winter (see Figure 1C); this abiotic categorization is also in agreement with reported October senescence patterns for *P. tremuloides* (Killingbeck et al., 1990). Differences were analyzed using a two-way ANOVA test.

Meteorological data

Weather data were provided by Alberta Agriculture and Forestry, Alberta Environment and Parks and Environment Canada, recorded from the Edmonton South Campus UA weather station.

RESULTS

Seasonal changes in callose deposition (Figure 1A) were less distinct compared to patterns described for xylem (Figure 1B). However, there was one similarity between the xylem and phloem patterns: callose deposition was lowest in early July 2019, with a maximum of only 7% of plates with callose deposition in *C. cornuta* and *S. aucuparia*. This timing coincided with the peak of the growing season and the time when xylem embolism was also uniformly low. At all other times of the year, callose deposition was more variable across species and tended to be more pronounced than in July.

There was no clear ranking across species in terms of the proportion of sieve plates with callose deposition. No significant difference in callose deposition was found when testing between species ($F_{4,30} = 0.9426$, $p = 0.45294$) or between sample month ($F_{6,28} = 1.8952$, $p = 0.1169$). No interaction was found between species and month ($F_{4,25} = 1.122$, $p = 0.3686$). Overall, deposition did not follow an obvious seasonal trend nor were there differences between any of the

five species observed in this study. In plates that did have callose deposition, deposition occurred around the edges of pores. In more heavily callosed plates, deposition almost entirely occluded individual pores where only a small opening in the center was seen. In other cases, most pores on a plate were completely covered in callose. However, many plates in the winter category had sieve plate pores free of callose. It should be noted that at each time interval, the data recorded are aggregates of three separate individuals. Some individuals had callose deposition on all plates, with no fully open pores. Sample size per individual was relatively low ($N = 5$). A more robust sample size would increase statistical power and lower the potential influence of outliers.

Meanwhile, there were distinct seasonal changes in xylem embolism (Figure 1B). Xylem embolism was minimal in June and July and increased at the end of the growing season. The highest embolism values were found in mid-winter after plants had experienced temperatures below –30°C and various freeze–thaw cycles. In April 2019, before leaf flush, three species had low embolism levels (*A. negundo*, *C. cornuta*, and *P. tremuloides*), while two species showed 44% and 53% embolism (*S. aucuparia* and *C. sericea*, respectively). These two species also showed the highest embolism values (~80%) in mid-winter.

The maximum and minimum daily temperatures are displayed for the 2019–2020 timeframe when xylem embolism and sieve plate data were collected (Figure 1C). From April to October 2019, mean daily temperatures stayed above freezing, denoted here as summer. In contrast, from November 2019 to March 2020, daily mean temperatures were below freezing, or winter.

After testing between summer and winter months (Figure 2), we found no significant difference between species ($F_{4,5} = 0.9817$, $p = 0.493$) or season ($F_{1,8} = 3.2557$, $p = 0.2183$) in terms of seasonal callose deposition. Further, there were no statistically significant interactions between season and species on percentage of callose deposition ($F_{4,25} = 0.8922$, $p = 0.48317$).
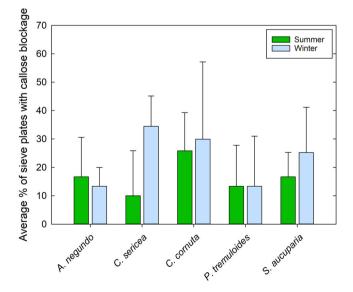
Cornus sericea had the highest variability between winter and summer with a peak of ~46% of plates with callose deposition during January 2020, while having none during April and July 2019. *Corylus cornuta* had the highest amount of plate deposition in January (53% of plates with deposition). However, an early November sampling collection for this species showed no detectable callose deposition. A similar pattern was observed for *P. tremuloides* where the early November sampling yielded the highest yearly deposition for this species (33%), but this pattern was completely reversed by the late January sampling (~7% of plates with deposition). Representative images of sieve plates are shown in Figure 3. Although most of the plates imaged had little callose deposition, some from the winter collections did have detectable amounts of callose (Figure 3, "winter", arrows). Other obstructions seemed to be remnants of p-protein that was not completely digested by the enzyme treatment.

Mean pore size per species was calculated (Table 1). Overall, the average pore diameters of the five species in this study vary between ~0.5–1 μm. The species with the smallest approximate mean pore area was *C. cornuta*, followed by *S. aucuparia*. The species with the largest approximate mean pore area was *P. tremuloides*, followed by *C. sericea* and *A. negundo*. Mean roundness (the ratio of mean minor axis [μm] to mean major axis [μm]) was calculated, where all five species maintained values between 0.6 and 0.7 (i.e., rather oblong pores were found). Due to the noncircular nature of the pores, the area of the pores is the most accurate representation of their hydraulic properties. However, to compare with previous work, which assumes round pores, estimated round pore diameters are also shown in Table 1.
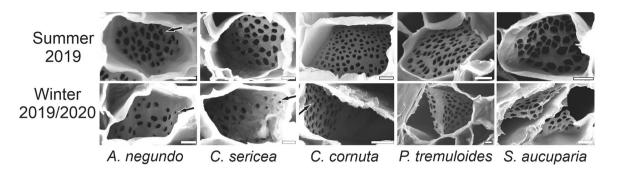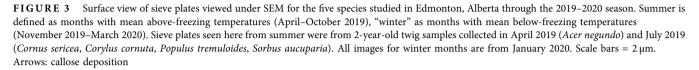
DISCUSSION

Trends in seasonal callose deposition

Our first objective was to quantify the percentage of phloem sieve plates that exhibited dormancy callose deposition for each species on a seasonal basis. The mean proportion of sieve plates with callose deposition was surprisingly low in winter, but still nonsignificantly higher than in summer. Davis and Evert (1968) suggested definitive callose is laid down in "massive quantities" in *P. tremuloides*, yet we observed consistently low callose deposition over winter for this species. However, our results are supportive of a previous report stating that *A. negundo* does not lay down definitive or dormancy callose (Tucker and Evert, 1969). Further, our results are supportive of Currier (1957) that the European species of dogwood does not lay down definitive

FIGURE 2 Mean (±SE) percentage of sieve plates with callose deposition per season. Summer: April–October 2019; Winter: November 2019–March 2020

FIGURE 3 Surface view of sieve plates viewed under SEM for the five species studied in Edmonton, Alberta through the 2019–2020 season. Summer is defined as months with mean above-freezing temperatures (April–October 2019), "winter" as months with mean below-freezing temperatures (November 2019–March 2020). Sieve plates seen here from summer were from 2-year-old twig samples collected in April 2019 (*Acer negundo*) and July 2019 (*Cornus sericea*, *Corylus cornuta*, *Populus tremuloides*, *Sorbus aucuparia*). All images for winter months are from January 2020. Scale bars = 2 μm. Arrows: callose deposition

TABLE 1 Descriptive statistics of sieve plate pores in the five study species. Mean major and minor axes, mean area per individual pore (μm²) per species, and SE of mean area (μm²), mean roundness of pores, and mean pore diameter. Mean roundness represents the ratio of the mean minor axis (μm) to mean major axis (μm). Measurements were taken of both axes using ImageJ software, and approximate area was calculated as $A = ab\pi$, where a is the semi-major axis and b is the semi-minor axis of the pore. For comparative purposes to prior literature, the pore diameter was estimated based upon the mean area of the pore, assuming that area came from a hypothetical perfectly round pore

Species	Mean major axis (μm)	Mean minor axis (μm)	Mean pore area (μm²)	SE pore area (μm²)	Mean roundness	Pore diameter (μm)
Acer negundo	0.959	0.591	0.459	0.040	0.623	0.764
Cornus sericea	1.171	0.708	0.668	0.054	0.630	0.922
Corylus cornuta	0.600	0.382	0.182	0.009	0.651	0.481
Populus tremuloides	1.236	0.815	0.795	0.041	0.662	1.000
Sorbus aucuparia	0.673	0.441	0.251	0.028	0.696	0.565

callose. In addition, we conclude that definitive callose is not laid down in *C. cornuta* and *S. aucuparia* because an inconsistent pattern of wintertime callose deposition was observed. However, future studies are needed for these species to determine whether the callose deposition we did find in mid-winter was instead dormancy callose. These studies could include assays (e.g., Knipfer et al., 2017) to determine the viability of sieve element/companion cell complexes over winter months.

However, our results trended toward a higher winter accumulation on plates in comparison to summer. It would be much more likely that abiotic or biotic environmental disturbances (Collinge and Slusarenko, 1987; Jaeger et al., 1988; Hao et al., 2008) may induce callose wound responses, all of which would be more likely in summer months. That we had higher rates of overall callose during the winter favors the idea that there was a small seasonal effect, but overall, callose-induced overwintering appeared minimal.

In many of the classic phloem studies (e.g., Alfieri and Evert, 1968; Tucker and Evert, 1969; Davis and Evert, 1970), sampling was dramatically different from the current study. For example, formalin acetic acid (FAA) was used instead of liquid nitrogen to arrest the development of callose in sieve plates. Liquid nitrogen is much more effective than FAA in arresting callose formation (Evert and Derr, 1964). Thus, previous work may have overestimated the amount of callose deposited in both definitive and dormancy callose strategies.

Our results agree with recent studies of *Populus balsamifera* (Montwé et al., 2019) and *Fagus sylvatica* (Prislan et al., 2018), which showed a minimal amount of callose accumulation during dormancy. If the fixation protocol did not bias the results of studies before 2010, then further sampling across many plant organs may prove promising to reconcile earlier results. Varying results between phloem collected from young shoot tips and mature boles may suggest that callose accumulation varies between different areas within the same individual.

Relating xylem and phloem seasonality

Overall, xylem embolism increased in all species throughout the growing season. By September, embolism levels ranged from 33–50% across species. This embolism increase was not caused by frost, nor was there an unusual degree of drought stress. The accumulated precipitation during the

growing season (1 April–30 September 2019) was 307 mm, which represents 91% of the long-term average recorded at this weather station (Edmonton South Campus UA). We therefore hypothesize that this embolism was caused by the most vulnerable vessels that may become dysfunctional at even mild levels of water stress. It is interesting that three species showed low xylem embolism values in April, before leaf flush, while two other species did not. In *A. negundo*, the low embolism level was likely due to the development of root and/or stem pressure in late winter and early spring (Sperry et al., 1988; Hacke and Sauter, 1996).

As an alternative to root pressure, Love and Sperry (2018) also found evidence for xylem refilling in *P. tremuloides*, and we refer readers to their discussion of this observation. During the growing season, water is exchanged between xylem and phloem (Pfautsch et al., 2015; Salleo et al., 2006). In spring, phloem is reactivated before the xylem in many species, as previously reported by Evert (2006) and Montwe et al. (2019). It is conceivable that some phloem activity is also required for the refilling of xylem vessels prior to the start of the growing season. The lack of a consistent callose blockage is compatible with this possibility.

Variability in sieve plate pores

Our third objective was to determine whether the area of sieve plate pores differs across species. It is interesting to note that despite *P. tremuloides* having a pore area >4× larger than *C. cornuta*, the callose deposition patterns did not obviously differ between species. Thus, pore size itself may not be a contributing factor toward overall callose deposition pattern, despite evidence that smaller diameter pores occlude faster after wounding (Mullendore et al., 2010).

Pore sizes seen here are much smaller than those from previous work. Zahur (1959) reported pores of 2.4 μm diameter in the secondary phloem of Cornelian cherry dogwood (*Cornus mas*), which is more than double of what we recorded for dogwood (*Cornus sericea*; 0.9 μm). Stanfield et al. (2019) found average pore diameters in *Populus balsamifera* to be 0.7 μm, which more closely follows the 1 μm average in *Populus tremuloides* found here; their study and ours sampled from twigs of the same age. For three other temperate woody species, Thompson and Holbrook (2003) reported sieve plate pore diameters of 2.5 μm for *Robinia pseudoacacia*, 1.2 μm for *Tilia americana*, and 4 μm for *Ulmus americana*.

The noticeably smaller pores we found in our study may be due to sampling location and plant size. For example, Clerx et al. (2020) found that sieve pore diameters in *Quercus rubra* changed drastically depending on (1) sampling location from the base and (2) the overall size of the tree from which the sample was collected. This association between tree height and sieve pore diameter has also been demonstrated over multiple taxa in a recent meta-analysis

(Liesche et al., 2017). Thus, along with variation due to differences between species, it is important to verify the location of where the secondary phloem was sampled to make comparisons valid.

AUTHOR CONTRIBUTIONS
The study topic was conceived by U.H. and R.S. and designed by A.M., R.S., and U.H. Phloem data were acquired by A.M. Phloem data were analyzed and interpreted by A.M. and R.S. Xylem data were acquired, analyzed, and interpreted by U.H. The manuscript was drafted by A.M., and revised by A.M., U.H., and R.S.

DATA AVAILABILITY STATEMENT
Data are archived and available on Zenodo (https://doi.org/10.5281/zenodo.4606019).

ORCID
Uwe G. Hacke http://orcid.org/0000-0001-5983-3582

REFERENCES
Alfieri, F. J., and R. F. Evert. 1968. Seasonal development of the secondary phloem in Pinus. *American Journal of Botany* 55: 518–528.

Aloni, R., and C. A. Peterson. 1991. Seasonal changes in callose levels and fluorescein translocation in the phloem of Vitis vinifera L. *IAWA Bulletin* 12: 223–234.

Bertoni, G. 2011. Dormancy cycling in Populus: the symplasmic connection. *Plant Cell* 23: 3.

Chen, X. Y., and J. Y. Kim. 2009. Callose synthesis in higher plants. *Plant Signaling & Behavior* 4: 489–492.

Clerx, L. E., F. E. Rockwell, J. A. Savage, and N. M. Holbrook. 2020. Ontogenetic scaling of phloem sieve tube anatomy and hydraulic resistance with tree height in Quercus rubra. *American Journal of Botany* 107: 852–863.

Collinge, D. B., and A. J. Slusarenko. 1987. Plant gene expression in response to pathogens. *Plant Molecular Biology* 9: 389–410.

Cronshaw, J., and K. Esau. 1968. P protein in the phloem of Cucurbita. *Journal of Cell Biology* 38: 292–303.

Currier, H. B. 1957. Callose substance in plant cells. *American Journal of Botany* 44: 478–488.

Davis, J. D., and R. F. Evert. 1968. Seasonal development of the secondary phloem in Populus tremuloides. *Botanical Gazette* 129: 1–8.

Davis, J. D., and R. F. Evert. 1970. Seasonal cycle of phloem development in woody vines. *Botanical Gazette* 131: 128–138.

Esau, K. 1948. Phloem structure in the grapevine, and its seasonal changes. *Hilgardia* 18: 217–296.

Esau, K. 1950. Development and structure of the phloem tissue. II. *Botanical Review* 16: 67.

Eschrich, W. 1975. Sealing systems in phloem. *In* M. H. Zimmerman and J. A. Milburn [eds.], Transport in plants I, Encyclopedia of plant physiology, vol. 1: 39-56. Springer, Berlin, Germany.

Evert, R. 1963. The cambium and seasonal development of the phloem in Pyrus malus. *American Journal of Botany* 50: 149–159.

Evert, R. 2006. Esau's plant anatomy: meristems, cells, and tissues of the plant body, 3rd ed. Wiley, Hoboken, NJ, USA.

Evert, R. F., and W. F. Derr. 1964. Callose substance in sieve elements. *American Journal of Botany* 51: 552–559.

Fadón, E., E. Fernandez, H. Behn, and E. Luedeling. 2020. A conceptual framework for winter dormancy in deciduous trees. *Agronomy* 10: 241.

Fisher, D. B. 1983. Year-round collection of willow sieve-tube exudate. *Planta* 159: 529–533.

Furch, A. C., M. R. Zimmermann, T. Will, J. B. Hafke, and A. J. van Bel. 2010. Remote controlled stop of phloem mass flow by biphasic occlusion in Cucurbita maxima. *Journal of Experimental Botany* 61: 3697–3708.

Hacke, U., and J. J. Sauter. 1996. Xylem dysfunction during winter and recovery of hydraulic conductivity in diffuse-porous and ring-porous trees. *Oecologia* 105: 435–439.

Hao, P., C. Liu, Y. Wang, R. Chen, M. Tang, B. Du, L. Zhu, and G. He. 2008. Herbivore induced callose deposition on the sieve plates of rice: an important mechanism for host resistance. *Plant Physiology* 146: 1810–1820.

Hillabrand, R. M., U. G. Hacke, and V. J. Lieffers. 2019. Defoliation constrains xylem and phloem functionality. *Tree Physiology* 39: 1099–1108.

Jaeger, C. H., J. D. Goeschl, C. E. Magnuson, Y. Fares, and B. R. Strain. 1988. Short-term responses of phloem transport to mechanical perturbation. *Physiologia Plantarum* 72: 588–594.

Killingbeck, K. T., J. D. May, and S. Nyman. 1990. Foliar senescence in an aspen (Populus tremuloides) clone: the response of element resorption to interramet variation and timing of abscission. *Canadian Journal of Forest Research* 20: 1156–1164.

Liesche, J., M. R. Pace, Q. Xu, Y. Li, and S. Chen. 2017. Height-related scaling of phloem anatomy and the evolution of sieve element end wall types in woody plants. *New Phytologist* 214: 245–256.

McNairn, R. B., and H. B. Currier. 1968. Translocation blockage by sieve plate callose. *Planta* 82: 369–380.

Mullendore, D. L., C. W. Windt, H. V. As, and M. Knoblauch. 2010. Sieve tube geometry in relation to phloem flow. *Plant Cell* 22: 579–593.

Peel, A. J. 1974. Transport of nutrients in plants. Elsevier, NY, NY, USA.

Pfautsch, S., J. Renard, M. G. Tjoelker, and A. Salih. 2015. Phloem as capacitor: radial transfer of water into xylem of tree stems occurs via symplastic transport in ray parenchyma. *Plant Physiology* 167: 963–971.

Prislan, P., P. Mrak, N. Žnidaršič, J. Štrus, M. Humar, N. Thaler, M. Tanja, and J. Gričar. 2018. Intraannual dynamics of phloem formation and ultrastructural changes in sieve tubes in Fagus sylvatica. *Tree Physiology* 39: 262–274.

Saguez, J., P. Giordanengo, and C. Vincent. 2013. Aphids as major potato pests. In A. Alyokhin, C. Vincent, and P. Giordanengo [eds.], Insect pests of potato, 31–63. Elsevier, NY, NY, USA.

Savage, J. A. 2020. It's all about timing—or is it? Exploring the potential connection between phloem physiology and whole plant phenology. *American Journal of Botany* 107: 848–851.

Sevanto, S., T. Hölttä, and N. M. Holbrook 2011. Effects of the hydraulic coupling between xylem and phloem on diurnal phloem diameter variation. *Plant, Cell & Environment* 34: 690–703.

Sperry, J. S., J. R. Donnelly, and M. T. Tyree. 1988. A method for measuring hydraulic conductivity and embolism in xylem. *Plant, Cell and Environment* 11: 35–40.

Stanfield, R. C., P. J. Schulte, K. E. Randolph, and U. G. Hacke. 2019. Computational models evaluating the impact of sieve plates and radial water exchange on phloem pressure gradients. *Plant, Cell & Environment* 42: 466–479.

Thompson, M. V. 2006. Phloem: the long and the short of it. *Trends in Plant Science* 11: 26–32.

Thompson, M. V., and N. M. Holbrook. 2003. Scaling phloem transport: water potential equilibrium and osmoregulatory flow. *Plant, Cell and Environment* 26: 1561–1577.

Thompson, M. V., and S. M. Wolniak. 2008. A plasma membrane-anchored fluorescent protein fusion illuminates sieve element plasma membranes in Arabidopsis and tobacco. *Plant Physiology* 146: 1599–1610.

Ton, J., and B. Mauch-Mani. 2004. Beta-amino-butyric acid-induced resistance against necrotrophic pathogens is based on ABA-dependent priming for callose. *Plant Journal* 38: 19–130.

Truernit, E. 2014. Phloem imaging. *Journal of Experimental Botany* 65: 1681–1688.

Tucker, C. M., and R. F. Evert. 1969. Seasonal development of the secondary phloem in Acer negundo. *American Journal of Botany* 56: 275–284.

Weatherley, P. E. and B. T. Watson. 1969. Some low-temperature effects on sieve tube translocation in Salix viminalis. *Annals of Botany* 33: 845–853.

White, P. J. 2012. Long-distance transport in the xylem and phloem. *In* P. Marschner [ed.], Marschner's mineral nutrition of higher plants, 3rd ed., 49–70. Elsevier, NY, NY, USA.

Wilhelm, K. 1880. Beiträge zur Kenntnis des Siebröhrenapparates dikotyler Pflanzen. Englemann, Leipzig, Germany.

Zahur, M. S. 1959. Comparative study of secondary phloem of 423 species of woody dicotyledons belonging to 85 families. Memoir 358, Cornell University Agricultural Experiment Station, Ithaca, NY, USA.

Zamski, E., and M. H. Zimmermann. 1979. Sieve tube longevity in white ash (Fraxinus americana) studied with a new histochemical test for the identification of sugar. *Canadian Journal of Botany* 57: 650–656.

Zhang, C., X. Yu, B. G. Ayre, and R. Turgeon. 2012. The origin and composition of cucurbit phloem exudate. *Plant Physiology* 158: 1873–1882.